Supplementary Material for
"**A type of robust superlattice type-I Weyl semimetals with four Weyl nodes**"

Lijun Meng⊠, Jiafang Wu, Jianxin Zhong and Rudolf A Römer⊠

Hunan Key Laboratory for Micro-Nano Energy Materials and Devices, Hunan, People's Republic of China

Faculty of Materials and Optoelectronic Physics, Xiangtan University, Xiangtan 411105, Hunan, People's Republic of China

Department of Physics, University of Warwick, Coventry, CV4 7AL, United Kingdom

1. Dynamic stability and formation energy for WTeS and WTeSe

In order to identify the dynamics stability of optimized structures, we conducted phonon dispersions for WTeS and WTeSe. In our calculations, we adopted plane-wave basis set and projector augmented wave method as implemented in the Vienna *Ab initio* Simulation Package (VASP) [1]. A plane-wave cutoff energy of 400eV, an energy convergence criteria of 1.0×10^{-6} eV and a Monkhorst-Pack mesh of $2 \times 1 \times 1$ are used in the supercell calculations. The harmonic interatomic force constants and dynamic matrices are obtained based on $4 \times 4 \times 1$ supercell by density functional perturbation theory (DFPT), which is realized in the PHONOPY code[2]. The phonon spectra along high symmetry path A-X-Γ-Z-A-Γ for WTeS and WTeSe are presented in Fig.1S. The absence of negative frequency in the phonon bands indicates that the WSeS and WTeSe are dynamically stable.
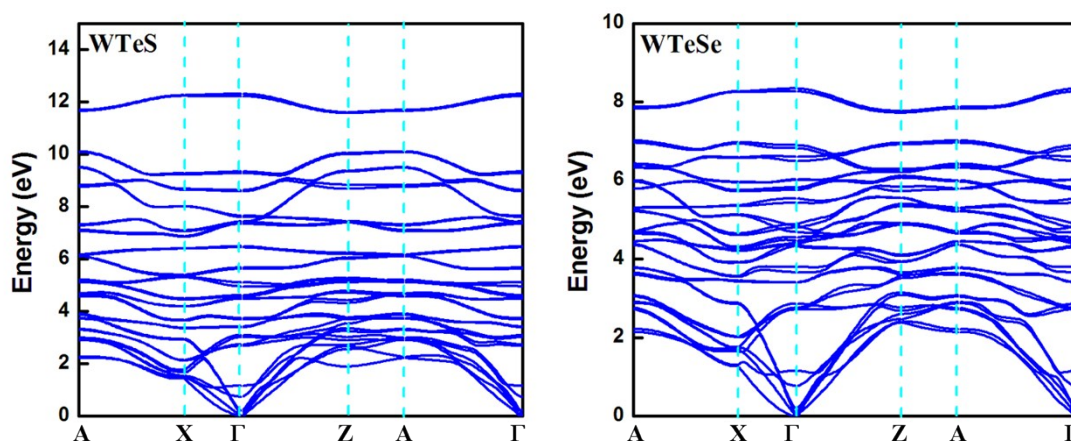
Fig.1S The phonon dispersions for WTeS and WTeSe.

The formation enthalpy ΔH_f plays an important role in modern material science[3, 4] The ΔH_f is defined as the change in enthalpy in a chemical reaction, which also is the energy needed to form a compound out of its elemental constituents. A negative ΔH_f usually

⊠ The corresponding author Email: ljmeng@xtu.edu.cn

⊠ The corresponding author Email: R.Roemer@warwick.ac.uk

implies that the examined compound is thermodynamically stable. At zero pressure and zero temperature, the formation enthalpy of a compound $A_{n1}B_{n2}\cdots$ is [3, 4]

$$\Delta H_f(A_{n1}B_{n2}\cdots) = E_{tot}(A_{n1}B_{n2}\cdots) - \sum_i n_i \mu_i^0 \quad , \quad (1)$$

where A, B,... reperesent the pure elements in their conventional reference phases and n_i stands for the number of atoms of the ith element in a single formula unit. $E_{tot}(A_{n1}B_{n2}\cdots)$ is the total energy per formula unit of a given compound and μ_i^0 are the total energies per atom of the elements A, B,... in their elemental reference phases. For compounds WTeS and WTeSe, we calculated the chemical potential (total energies) of pure elements S, Se, Te and W in their respective reference phases as given in Table.1S. The results are close to that of TABLE V in reference [3].

Table.1S Chemical potentials μ_i^0 of elements in their reference phases.

Elements	Reference phases	μ_i^0	PRB, **85** 115105(2012)
S	P3$_1$21(No.152)	-4.089	-4.00
Se	P3$_1$21(No.152)	-3.521	-3.55
Te	P3$_1$21(No.152)	-3.259	-3.25
W	Im3m (No.229)	-13.241	-

Table.2S. The enthalpy of formation for compounds in T$_d$ phase.

compounds	E_{tot}(eV)	ΔH_f(eV/Atom)
WS$_2$	-23.328	-0.886
WSe$_2$	-21.589	-0.759
WTe$_2$	-19.935	-0.409
WTeS	-21.467	-0.591
WTeSe	-20.696	-0.565

The enthalpies of formation for five compounds are obtained according to the equation (1) and are listed in Table.2S. First, the negative value of formation enthalpy for WTeS and WTeSe demonstrate the thermodynamics stability of both compounds. Second, we also calculated the formation enthalpy (energy) distance between WTeS (WTeSe) and WS$_2$/ WTe$_2$ (WSe$_2$/WTe$_2$). Consequently, we found the formation enthalpy ΔH_f for both WTeS and WTeSe are closer to the parent phase of WTe$_2$ which is well-known Weyl semimetal. The results give as follows:

For WTeS:

|-0.591(WTeS)-(-0.409(WTe$_2$))| =0.182 < |-0.591(WTeS)-(-0.886(WS$_2$))|=0.295

For WTeSe:

|-0.565(WTeSe)-(-0.409(WTe$_2$))|=0.156 < |-0.565(WTeSe)-(-0.759(WSe$_2$))|=0.194

2. The lattice constants and Brillouin zone for optimized WTeS and WTeSe

The lattice constants and atomic coordinates for optimized WTeS and WTeSe are presented in Table I in the text and Table.3S. The angle α in the monoclinic phase shows a small deviation compared with the pristine orthogonal T_d-phase with angle α=90°. The α angles for both structures are 91.81° and 91.20°, respectively, and lead to a slightly broken g_{xz} symmetry. The coordinates of high symmetry points in the Brillouin zone (BZ) of monoclinic phase depend the following two parameters η and v[5]

$$\eta = (1 - bcos\alpha/c)/(2sin^2\alpha),$$

$$v = (1/2 - \eta ccos\alpha)/b,$$

where the parameters b, c and α are lattice parameters which are given in Table.3S. We calculated the parameters η and v as follow:

For WTeS: η=0.507, v=0.535
For WTeSe: η=0.505, v=0.523

As a result, we obtained the coordinates of all high symmetry points (Table.4S). We take H and H_1 for examples in reduced unit:
For WTeS: H (0, 0.507, 0.465), H_1 (0, 0.493, 0.535)
For WTeSe: H (0, 0.505, 0.477), H_1 (0, 0.495, 0.523)

Table.3S Lattice parameters of optimized Janus superlattice structures of WTeS/Se in monoclinic phase with DFT-D3 VdW correction.

Systems	a(Å)	b(Å)	c(Å)	α(°)	$\beta=\gamma$(°)
WTeS	3.321±0.003	6.030±0.003	13.13±0.04	91.81±0.06	90.00
WTeSe	3.381±0.002	6.122±0.002	13.67±0.03	91.20±0.01	90.00

Table. 4S The high symmetry k-points of monoclinic phase[5].

k-points	$\times b_1$	$\times b_2$	$\times b_3$	k-points	$\times b_1$	$\times b_2$	$\times b_3$
Γ	0	0	0	H_2	0	η	-v
A	0.5	0.5	0	M	0.5	η	1-v
C	0	0.5	0.5	M_1	0.5	1-η	v
D	0.5	0	0.5	M_2	0.5	η	-v
D_1	0.5	0	-0.5	X	0	0.5	0
E	0.5	0.5	0.5	Y	0	0	0.5
H	0	η	1-v	Y_1	0	0	-0.5
H_1	0	1-η	v	Z	0.5	0	0

We calculated energy bands along high-symmetry path A-X-Γ-Z-A-Γ and he specific of high-symmetry points[5] are given in Table 5S.

Table 5S. The k point coordinates of high symmetry points in our calculations.

k-points	$\times b_1$	$\times b_2$	$\times b_3$
Γ	0.0	0.0	0.0

Z	0.5	0.0	0.0
X	0.0	0.5	0.0
A	0.5	0.5	0.0

3. The bands along the k_x, k_y and k_z axes around one of Weyl nodes

To verify the Weyl node is type I Weyl node, we calculated the bands along the k_x, k_y and k_z axes around one of Weyl nodes as shown in Fig.2S. According to the previous argument, there is a point-like of contact between the conduction band(CB) and valence band(VB) and form a closed point-like Fermi surface which is a manifestation of type I Weyl nodes[6]. In order to display clearly the point-like Fermi surface, we calculated the bands along the three axes (k_x, k_y and k_z) as shown in the Fig.2S. It's easy to see from the Fig.2S that the CB (red line) and VB (black line) intersect at one point and results in a twofold degenerated Weyl node with a closed Fermi surface for both WTeS and WTeSe.
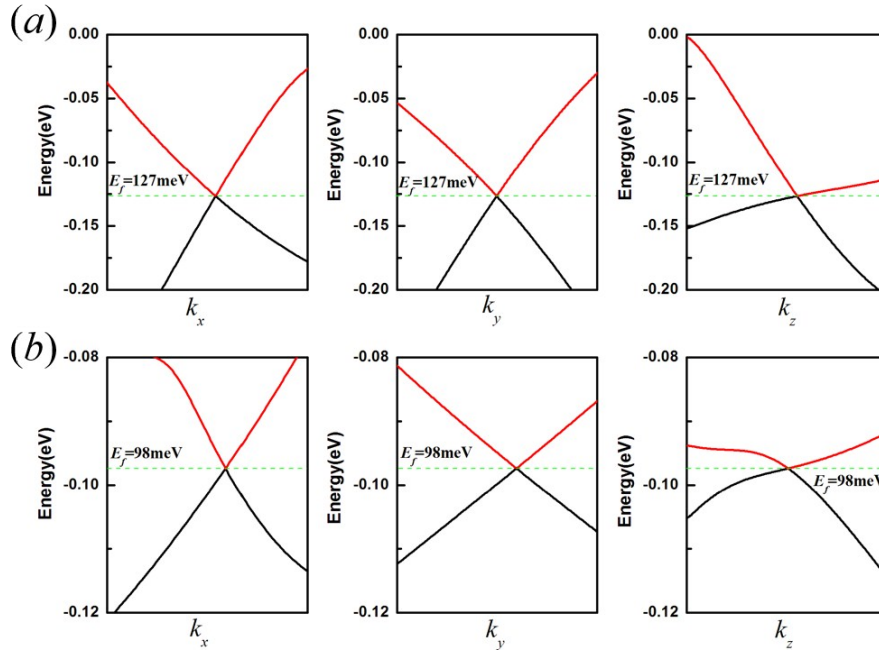
Fig.2S The bands along k_x, k_y and k_z axes around one of Weyl points. (*a*)WTeS; (*b*) WTeSe. The green dash line represent the Fermi level.

References

1.   G. Kresse and J. Furthmu¨ller, *PHYSICAL REVIEW B*, 1996, **54**, 11169.
2.   A. Togo and I. Tanaka, *Scripta Materialia*, 2015, **108**, 1-5.
3.   V. Stevanović, S. Lany, X. Zhang and A. Zunger, *Physical Review B*, 2012, **85**, 115104.
4.   R. Gautier, X. Zhang, L. Hu, L. Yu, Y. Lin, T. O. L. Sunde, D. Chon, K. R. Poeppelmeier and A. Zunger, *Nature Chemistry*, 2015, **7**, 308-316.
5.   W. Setyawan and S. Curtarolo, *Computational Materials Science*, 2010, **49**, 299-312.
6.   A. A. Soluyanov, D. Gresch, Z. Wang, Q. Wu, M. Troyer, X. Dai and B. A. Bernevig, *Nature*, 2015, **527**, 495-498.